Available online at www.sciencedirect.com

ScienceDirect

Energy Procedia 49 (2014) 579 – 588

Energy Procedia

SolarPACES 2013

CFD analysis of a receiving cavity suitable for a novel CSP parabolic trough receiver

S.A. Zavattoni[a], A. Gaetano[a], M.C. Barbato[a,*], G. Ambrosetti[b], P. Good[c], F. Malnati[b], A. Pedretti[b].

[a]*Department of Innovative Technologies, SUPSI, Manno 6928, Switzerland.*
[b]*Airlight Energy Manufacturing SA, Biasca 6710, Switzerland*
[c]*Department of Mechanical and Process Engineering, ETH Zurich, 8092 Zurich, Switzerland.*

Abstract

The aim of this work was to study, by means of accurate 3D steady-state CFD simulations, the thermo-fluid dynamics behavior of a helically coiled heat exchanger (HCHE) constituting the receiving cavity of the novel CSP receiver based on Airlight Energy technology. In this innovative receiver design, air is used as heat transfer fluid (HTF), which, besides being inexpensive and environmentally friendly, is optimally suited for high temperature operation well beyond the limit of conventional HTFs.
According to preliminary information related to the collectors orientation of the first 3.9 MW_{th} Airlight Energy pilot plant, under construction in Ait Baha (Morocco), two reference skew angles of the incoming solar radiation were considered and the receiving cavity performance were evaluated in terms of thermal efficiency and pressure drop. Among all, one of the main requirements was to achieve, at the outlet section of the HCHE, an air temperature of 650°C; hence the mass flow rate was tuned accordingly.
In order to minimize the pumping power requirements, the HCHE was designed to guarantee a laminar flow regime under all the operating conditions. Navier-Stokes, energy and radiation transport equations, the latter accounted for by the Discrete Ordinates (DO) model, were numerically solved, using the finite-volume method approach, with Fluent code from ANSYS.
A meticulous experimental proof of concept was then carried out in Biasca (Switzerland) by the Swiss company Airlight Energy Manufacturing SA. The analysis of the experimental results, detailed in this paper, allowed to assess the reliability and effectiveness of this novel CSP receiver design in the solar energy harvesting.

Selection and peer review by the scientific conference committee of SolarPACES 2013 under responsibility of PSE AG.
Final manuscript published as received without editorial corrections.

Keywords: receiving cavity, helically coiled heat exchanger (HCHE), heat transfer, computational fluid dynamics (CFD), air receiver.

* Corresponding author. Tel.: +41 058 666 6639.
E-mail address: maurizio.barbato@supsi.ch

Selection and peer review by the scientific conference committee of SolarPACES 2013 under responsibility of PSE AG.
Final manuscript published as received without editorial corrections.
doi:10.1016/j.egypro.2014.03.062

1. Introduction

With the aim of overcoming the limitations of conventional parabolic trough in concentrating solar power (CSP) systems for large-scale solar electricity production, Airlight Energy has developed a completely new CSP solution based on an inflated mirror trough collector with precast fiber-reinforced concrete sustaining structure The multi-arc pneumatic mirror system allows to achieve the focusing characteristics of a parabolic trough with high optical efficiency while the concrete sustaining structure provides a rigid frame that can be easily manufactured on-site, all leading to a very low collector cost per primary aperture area [1]. The left-hand side of Fig. 1 depicts a schematic of the new solar collector.

A novel approach has also been followed for the receiver design, which includes an additional concentration stage, in turn coupled to a string of helically coiled heat exchangers exploited as cavity receivers. Air is used as heat transfer fluid (HTF), which, besides being inexpensive and environmentally friendly, is optimally suited for high temperature operation, above 650°C, and enables the use of a low-cost rock bed thermal energy storage (TES) system [2].

The whole receiver and the inflated mirrors are separated from the external environment by a thin ethylene tetrafluoroethylene (ETFE) top-sheet widely used in building applications. Beyond the intrinsic advantages provided such as: remarkable corrosion resistance, temperature resistance, self-cleaning and good optical properties (total transmittance for solar radiation of 92%), the ETFE layer allows to minimize the mirrors reflecting reduction, due to dust deposition, creating a clean and controlled environment.

All these innovations will equip the first 3.9 MW_{th} pilot plant, under constructions, in Ait Baha (Morocco). The right-hand side of Fig. 1 shows a rendering of the three full-scale collectors, 211.68 m long, of the plant.

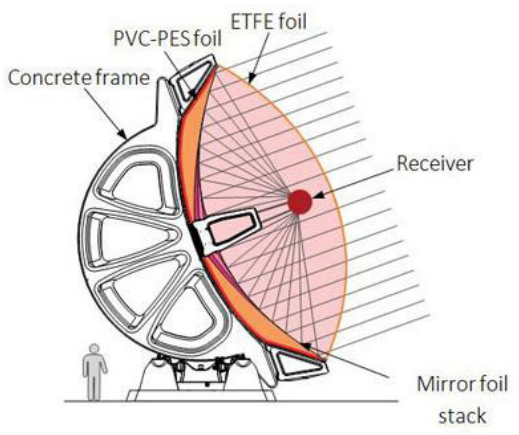

Fig. 1. Schematic of the solar collector (l.h.s.); rendering of the 3.9 MW thermal Ait Baha pilot plant (r.h.s.). Courtesy of Airlight Energy Manufacturing SA.

2. Working principle of the novel CSP receiver based on Airlight Energy Technology

A schematic cross-section of the novel receiver design is given in Fig. 2. Solar energy is collected and focused by the primary optics (multi-layer stack of aluminized polymer membranes) towards the receiver where a secondary hyperbolic concentrator allows to avoid potential dispersion of energy directing it into the receiving cavities through a glass window treated with a special broadband anti-reflective (AR) coating to minimize reflection losses. The external surfaces of this high-efficiency optics are coated with a thin aluminum film maximizing the reflectivity behavior. In order to maintain the favorable optics characteristics, the coating cannot withstand temperatures higher than 120°C; therefore, a water-cooling system is provided to maintain the aluminum structure of the secondary optics into a safety temperature range. The overall geometric concentration ratio obtained is in the order of 97 Suns.

The core of this innovative receiver is well represented by the helically coiled heat exchangers (r.h.s. of Fig. 2), which constitute the receiving cavities. The high density solar energy hits the inner surfaces of the cavities and is then gathered, in the form of thermal energy, by the heat transfer fluid (air) which is fed into the receiver from the bottom, by two feeding pipes, at low temperature (120°C) and pressure slightly above the atmospheric. Air at high temperature (up to 650°C), coming from all the cavities, is then collected into a single 450 mm diameter run-back pipe and used to feed both the steam generators and the high temperature rock-bed TES system.

In the Ait Baha (Morocco) pilot plant, a total of three full-scale collectors will be built. The overall collector length is obtained assembling 36 standard modules with an active mirror surface of 57 m^2 each leading to a total reflecting area of 2,053 m^2 for every collector.

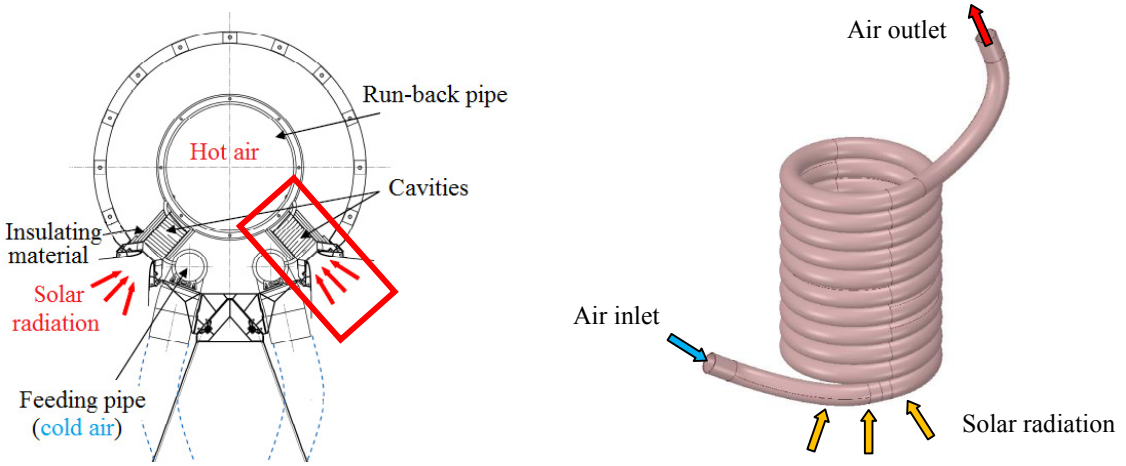

Fig. 2. Schematic cross-section of the novel receiver design (l.h.s.); receiving cavity and secondary optics magnification (r.h.s.).

3. Helically coiled heat exchangers (HCHEs)

Internal flows in helically coiled pipes have been extensively studied, [3-6], because of their wide use in industry. In particular, coiled tubes are interesting for heating and cooling applications because the centrifugal force causes a secondary flow consisting in a pair of counter-rotating vortices, also known as Dean effect [7], which leads to a twofold advantage with respect to straight tubes: 1) an enhanced heat transfer coefficient, for the same flow conditions, without causing excessive pressure drop as it occurs e.g. in turbulent flows; 2) and a stabilizing effect on the flow regime moving forward the critical Reynolds number from laminar to turbulent transition.

Therefore, thanks to the various advantages offered, in this innovative CSP receiver design, HCHEs are exploited to harvest the incoming solar radiation.

In order to keep the pumping power demand at a low level, the HCHE was designed in such a way that the flow regime into the pipe stays laminar under all operating conditions.

Being a high temperature application, stainless steel was selected as material of the pipe used to produce the helical coils. The external surface of the steel pipe was painted with a special black paint maximizing the solar energy absorption behavior and hence the overall heat transfer. Right-hand side of Fig. 2 depicts a schematic of the receiving cavity working principle.

The characteristics geometric parameters of the HCHE have been carefully analyzed, by means of a purpose-built analytical model, based upon the work of Manlapaz and Churchill [8, 9], together with accurate computational fluid dynamics (CFD) simulations, in order to find the optimum trade-off between manufacturability, heat transfer efficiency and overall pressure drop.

The final optimized HCHE dimensions are: 11 mm internal pipe diameter, an average helix diameter of 80 mm for a total of 10 coils.

For the industrial-scale application, a total of about 4,600 receiving cavities are used to cover the whole collector length of 211.68 m (2,300 receiving cavities linearly assembled along each side).

4. Ait Baha pilot plant – Collectors orientation

Because of the ground conformation, the collectors of the Ait Baha pilot plant cannot be perfectly oriented towards the north-south direction. This leads to the fact that the receiver will always operate with a certain skew angle, i.e. the inclination of incoming solar radiation with respect to the direct normal irradiation (DNI) condition, different from zero. According to preliminary investigations, with the given misalignment, the receiver will mostly operate within two skew angle limits of 18° and 40°. Wider skew angles are not of particular interest since the solar concentration decreases rapidly due to end-losses (i.e. fraction of energy, reflected from the primary optics, that falls beyond the receiver [10]) and longer travel paths of the rays from the point of their reflection on the primary mirrors to the point of their absorption.

The skew angle effect was considered applying the relative input power only to the internal HCHE surfaces which are actually irradiated. The exact energy distribution was obtained from ray-tracing simulations. Based upon the latter, the reference skew angles were modeled with the following energy distribution:

- Skew 18°: the incoming solar radiation hits half of the HCHE internal surfaces and a small fraction of the cover at the top. According to the ray-tracing analysis, the input power hitting the HCHE surfaces is equal to 333.6 W.

- Skew 40°: at this skew angle, the incoming solar radiation hits only a quarter of the internal surface with a linearly decreasing intensity from the maximum near the internal glass surface. The input power hitting the HCHE surfaces is equal to 253.9 W.

5. CFD modeling and numerical details

In order to provide useful information for the first pilot plant, the thermal behavior of the receiving cavity was analyzed by means of 3D steady-state CFD simulations. It was examined under realistic working conditions in terms of collector orientation, available DNI and air outlet temperature. Concerning the latter, the main requirement was to achieve 650°C at the HCHE outlet section; therefore, the inlet mass flow rate was tuned accordingly. Due to the high receiver complexity, the CFD analysis was limited to the region, highlighted in red, on the l.h.s. of Fig. 2.

Figure 3 depicts the computational domain considered. It was discretized with a grid of 6,450,000 hexahedral cells. The receiver is composed by a linear string of cavities, therefore, in order to simulate the thermal behavior of a representative HCHE, far from its edge, periodic boundary conditions were used to numerically model the presence of other receiving cavities before and after the actual computational domain.

Since the air flow velocity is relatively small, i.e. the Mach number is much lower than the threshold of 0.3 [11], and no relevant pressure variations are expected, the compressibility effects on the air flow are considered negligible. The air flow regime into the HCHE is laminar.

Radiative heat transfer was accounted for by the Discrete Ordinates (DO) model [12, 13]. Navier-Stokes, energy and radiation transport equations were numerically solved with Fluent code from ANSYS. The numerical solution of governing equations was performed with the “pressure-based” approach, which assumes that mass density depends on temperature and on a fixed pressure reference value [14].

The SIMPLE (Semi-Implicit Method for Pressure-Linked Equations) algorithm [15, 16] was used as pressure-velocity coupling scheme.

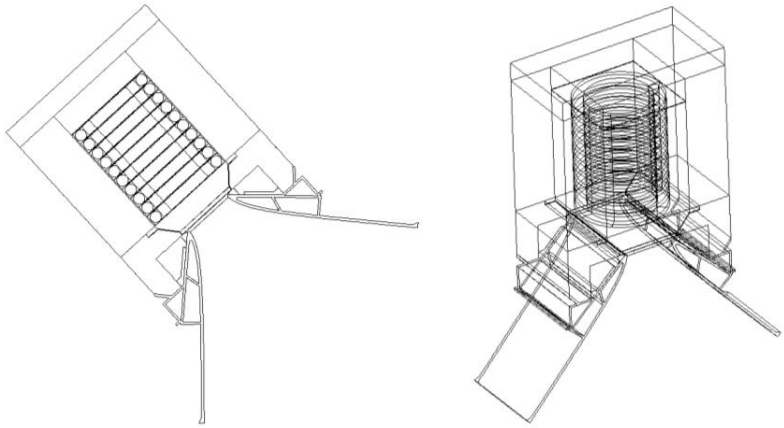

Fig. 3. Front and perspective views of the computational domain considered.

The CFD simulations were performed on a Linux Cluster with AMD multicore processors. All model equations were solved with second order upwind numerical schemes [17]. Convergence was considered achieved when dominant mass fractions residuals were below 10^{-5}, energy and radiation intensity residuals were below 10^{-9} and 10^{-6} respectively.

5.1. Physical properties of the materials involved

Thermo-physical properties of air (specific heat, thermal conductivity and viscosity) were assigned as piecewise linear interpolations of tabulated data available in the literature [18]. Instead, thermal properties of solid materials (ceramic, calcium silicate, steel and aluminum), were obtained from the manufacturers data sheets and assigned as constant values. Thermal conductivities of Microtherm® insulating material and Borofloat® glass were modeled as piecewise linear profile as indicated by the suppliers [19, 20].

6. CFD simulations – Input parameters and results

Two different CFD simulations were run changing the incoming solar energy distribution according to the two reference skew angles working conditions. Table 1 provides an overview of both the HCHE geometric details and the main boundary conditions used to set the CFD simulations.

In order to account for heat losses, a conservative 8 $W/(m^2 \cdot K)$ was computed as convective heat transfer coefficient (HTC). Wind does not directly affect the HTC since the ETFE top-sheet protects the receiver from the external environment (see l.h.s. of Fig. 1). Based upon preliminary computations, the temperature of this controlled environment was considered equal to 70°C. As far as concerning its optical properties [21], albeit ETFE is not completely opaque to long-wave radiation, the fraction of energy transmitted into this range is very small and therefore it can be safely neglected. With this assumption, the environment temperature used to compute the radiative heat transfer was set equal to the ETFE equilibrium temperature (70°C) instead of the sky temperature (5°C).

The heat losses from the external glass surface are given by conduction and thermal radiation; the contribution given by natural convection was neglected since, according to preliminary CFD simulations, it is very low and hence, the effect of gravity was not taken into account.

Table 1. HCHE characteristic dimensions and main boundary conditions applied to the model.

Input data		
Geometric details:		
average helix diameter	0.08	[m]
external helix diameter	0.092	[m]
coiled pipe internal diameter	0.011	[m]
coiled pipe length	2.5	[m]
number of coils	10	[-]
Boundary conditions:		
air inlet temperature	120	[°C]
external convective heat transfer coefficient	8	[W/(m^2·K)]
controlled environment temperature	70	[°C]
radiation temperature	70	[°C]
water-cooling circuit mass flow rate	$1.5 \cdot 10^{-3}$	[kg/sec]
water-cooling circuit inlet temperature	65	[°C]

The main CFD simulations results obtained, for both the cases analyzed, are reported in Table 2. Since the requirement was to achieve 650°C air temperature at the HCHE outlet section, the air inlet mass flow rate was computed based upon: inlet and outlet temperature, incoming solar radiation and heat losses estimation with the analytical model. The effectiveness of the receiving cavity in the harvesting and conversion of the incoming solar radiation was evaluated computing the radiation-to-thermal efficiency. The latter is defined as the amount of power removed by the HTF divided by the input power hitting the HCHE internal surfaces.

Table 2. CFD simulations results for the two reference skew angles.

	skew 18°	**skew 40°**	
mass flow rate	$4.7 \cdot 10^{-4}$	$2.83 \cdot 10^{-4}$	[kg/sec]
input power	333.6	253.9	[W]
Temperature:			
air outflow	655.3	626.5	[°C]
cavity maximum	682.4	718.8	[°C]
glass external surface	363.4	449.7	[°C]
Pressure:			
pressure drop	876	470	[Pa]
pressure drop per unit length	350	188	[Pa/m]
Power:			
removed by the air-flow	269.2	153.7	[W]
lost from the glass external surface	42.4	70.2	[W]
cooling circuit	31.3	42.6	[W]
Efficiency:			
expected optical efficiency	78.6	74.3	[%]
radiation-to-thermal efficiency	**80.7**	**60.5**	**[%]**

The power distribution analysis allows to clearly understand the performance of the system. With the given assumptions, a total of about 81% and 60.5% of the incoming solar radiation hitting the HCHEs internal surfaces were gathered by the HTF for the skew 18° and skew 40° working conditions respectively.

From a graphic standpoint, the resulting temperature distribution is reported, for both the skew angles working conditions, by Fig. 4 and Fig. 5.

Figure 4 depicts the temperature distribution of the receiving cavity internal walls and the internal glass surface. The left-hand side of Fig. 4 is relative to the skew 18° working conditions. In this case, the incoming solar radiation hits the HCHE as follows: 28.4% onto the bottom part of the first coil directly illuminated; 58.6% onto half of the internal surfaces of the coils for the whole cavity height; while, the last 13%, onto the metal sheet at the top of the helix. A large fraction of the internal surfaces are hit by the incoming solar radiation leading to a favorable condition for heat transfer. Furthermore, back-radiation losses are minimized since the hot region of the cavity is far enough from the glass window. The lowest temperature, at the bottom of the HCHE, indicates the effective cooling due to the low temperature of the HTF at the entrance region.

The Right-hand side of Fig. 4 shows the temperature distributions in the case of skew 40° working condition. Here, the incoming solar energy distributes, according to the geometric characteristics of the HCHE, as follows: again 28.4% onto the bottom part of the first coil, while, the remaining 71.6% onto a quarter of the internal HCHE surfaces for a total height of 7 coils. This different distribution has a negative impact on the heat transfer. Even though the total amount of energy entering the receiving cavity is lower than the previous case, it is focused onto a smaller surface area leading to a hot spot creation. Moreover, the hottest region of the receiving cavity is closer to the glass window bringing to a remarkable increment of the heat losses due to conduction and back radiation. Hence, the combination of these two side effects leads to a total of 20% reduction of the receiving cavity radiation-to-thermal efficiency with respect to the previous case.

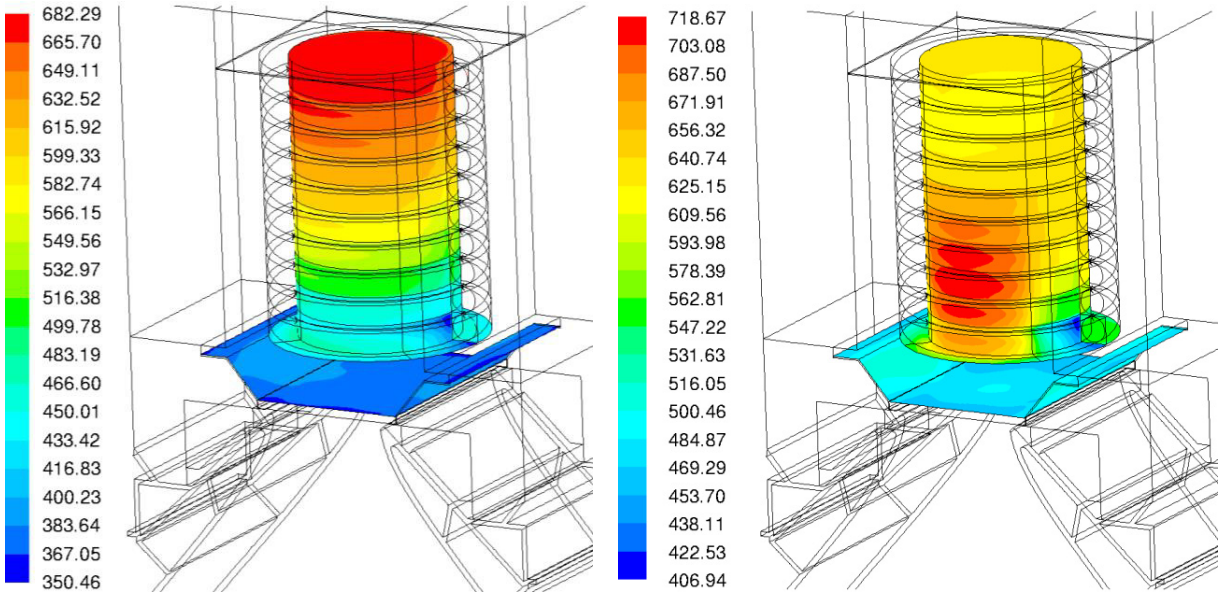

Fig. 4. Temperature distribution of receiving cavity and internal glass surface in the case of skew 18° (l.h.s.) and skew 40° (r.h.s.) working conditions. Temperature values are in [°C].

Figure 5 depicts the temperature contours onto the HCHE middle plane in the case of skew 18° (l.h.s.) and skew 40° (r.h.s.) working conditions. These two figures allow to visualize the temperature gradient for the whole model.

A fixed-temperature boundary condition, of 650°C, was selected to model the influence of the run-back pipe, onto the cavity thermal behavior, in the upper part of the computational domain. The visual comparison of the two cases shows, in the case of skew 40°, the higher temperature in the bottom region of the receiving cavity. This leads to a sensible increment of the heat losses through the glass window (see Table 2).

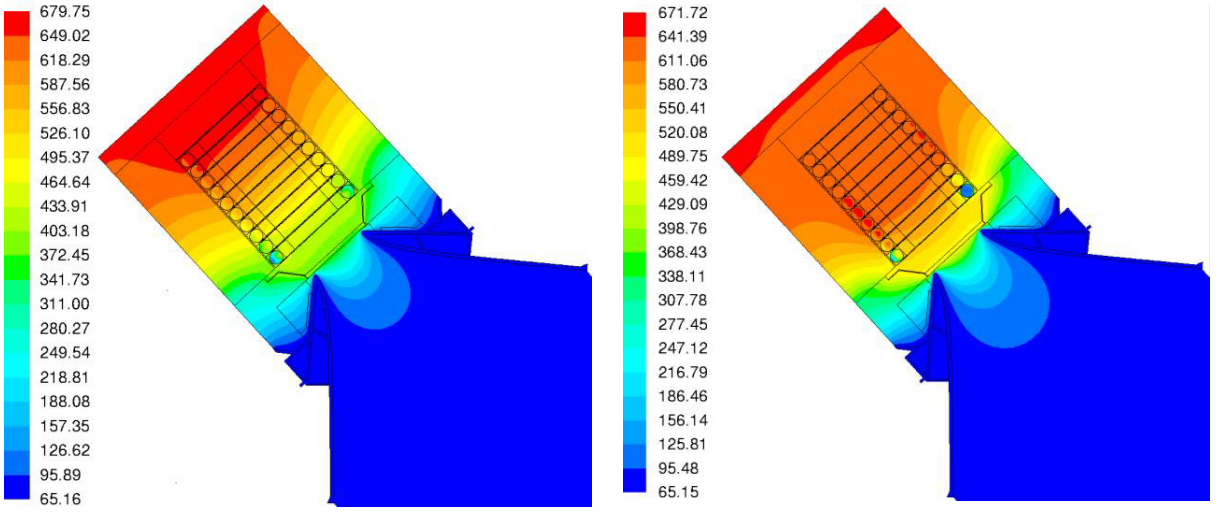

Fig. 5. Contours of temperature in the case of skew 18° (l.h.s.) and skew 40° (r.h.s.) working conditions. Temperature values are in [°C].

7. Experimental proof of concept

A meticulous experimental proof of concept has been carried out on October 16th 2013 in Biasca (CH), by the Swiss company Airlight Energy Manufacturing SA, demonstrating the effectiveness of this novel CSP receiver design in the solar energy harvesting. The test rig (1.38 m long, 0.44 m wide and 0.53 m high) was composed by: a) 5 stainless steel HCHEs, linearly positioned next to each other; b) a glass window with broadband AR coating; c) pipes to feed and to collect the air from the receiving cavities; d) Microtherm® insulating material and e) an external box to enclose all the components.

The test rig was also equipped with flow meters (air and water) and a total of 36 K-type (Chromel – Alumel) thermocouples (TCs), with an operative range from -200°C to 1,200°C, in order to monitor and record the temperature of the air at the inlet and outlet sections of the HCHEs and the temperature of some other zones of interest. The thermal acquisition system allowed to record the temperatures every 10 seconds with an accuracy of 2°C.

Solar energy was collected by means of a solid primary mirror with the same useful area of the new developed industrial-scale multi-arc pneumatic mirror. The primary mirror was composed by four different segments, laid onto a steel structure, leading to an aperture of 4.85 m and a length of 1.2 m wide. A secondary hyperbolic concentrator, with the relative water-cooling circuit, was installed below the receiving cavities. The test rig was then assembled, onto the steel structure, at the primary mirror focal point.

Figure 6 shows the test rig assembled on the two-axis tracking system and a magnification of the receiving cavities hit by solar radiation during the experimental campaign.

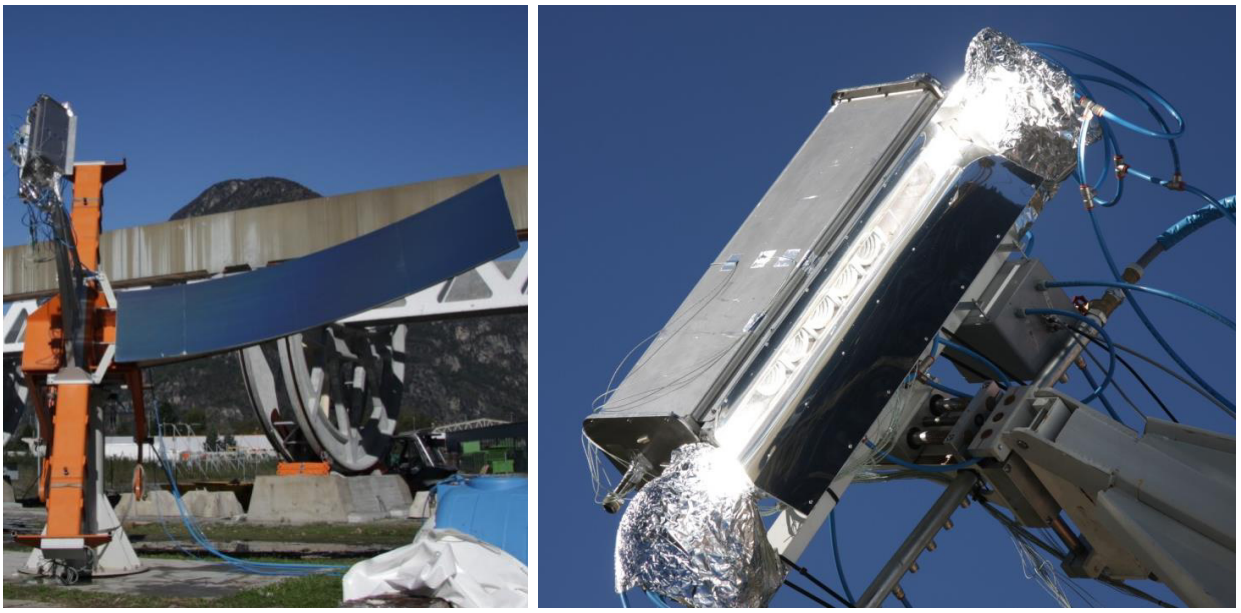

Fig. 6. Test rig assembled on the two-axis tracking system with primary mirror (l.h.s.); magnification of the receiving cavities with the secondary optics (r.h.s.). Courtesy of Airlight Energy Manufacturing SA.

The prototype was tested varying the air inlet mass flow rate in order to analyze its thermal response and to demonstrate its capability of withstanding the operating condition. The average DNI during the experiment was about 900 W/m^2 and the highest air outlet temperature, reached at the outlet section of the HCHE 5, was 630°C.

8. Conclusions

The thermo-fluid dynamics behaviour of the HCHE, exploited as receiving cavity to collect the incoming solar radiation, was studied by means of accurate 3D steady-state CFD simulations under two different skew angle working conditions, of 18° and 40° respectively, given by the collectors orientation of the first pilot plant under construction in Ait Baha (Morocco).

The CFD simulations results showed that the HCHE can be effectively exploited as receiving cavity to capture and transfer the incoming solar radiation to the HTF. With the given assumptions and approximations, a theoretical solar-to-thermal energy efficiency of 63.4%, with air outlet temperature from the HCHE of 655.3°C, was obtained for the most favourable working condition of skew 18°.

The 20% of efficiency difference between the two cases is due to the different distribution of the incoming solar radiation onto the internal HCHE surfaces which leads to heat losses increase and, at the same time, to a worsening of heat transfer.

Based on the CFD results, an experimental test rig was built and an experimental proof of concept was carried out, on October 16th 2013, by Airlight Energy Manufacturing SA. This on-field test showed the effectiveness of this novel CSP receiver design that delivered high temperature air up to 630°C.

Acknowledgements

This work has been developed in the framework of the SolAir-2 and SolAir-Pilot Projects (project “SI/500091” and “SI/500508”) financed by the Swiss Federal Office of Energy (SFOE - OFEN - BFE) under the contract numbers “SI/500091-01” and “SI/500508-01” respectively.

References

[1] Pedretti A., "A 3 MW thermal concentrated solar power pilot plant in Morocco with the Airlight Energy technology" SolarPACES 2012, Marrakech, Morocco.
[2] Zavattoni S., Barbato M., Pedretti A., Zanganeh G., Steinfeld A., "Effective thermal conductivity and axial porosity distribution of a rock-bed TES system: CFD modeling and experimental validation" SolarPACES 2012, Marrakech, Morocco, Paper ID 23336.
[3] Yasuo M., Nakayama W., "Study on forced convective heat transfer in curved pipes (1st report, laminar region)", International Journal of Heat and Mass Transfer Vol. 8, Issue 1, pp. 67–82, 1965.
[4] Mori Y., Nakayama W., "Study of forced convective heat transfer in curved pipes (2nd report, turbulent region)", International Journal of Heat and Mass Transfer Vol. 10, Issue 1, pp. 37-59, 1967.
[5] Tarbell J.M., Samuels M.R., "Momentum and heat transfer in helical coils", Chemical Engineering Journal Vol. 5, Issue 2, pp. 117–127, 1973.
[6] Berger S.A., Talbot L., Yao L.S., "Flow in curved pipes", Annual Review of Fluid Mechanics Vol. 15, pp. 461-512, 1983.
[7] Dean W.R., "The stream-line motion of fluid in a curved pipe", Philosophical Magazine 7, Vol. 5, Issue 30, pp. 673-695, 1928.
[8] Manlapaz, R.L., Churchill, S.W., "Fully developed laminar flow in a helically coiled tube of finite pitch", Chemical Engineering Communications 7, pp. 57-78, 1980.
[9] Manlapaz, R.L., Churchill, S.W., "Fully developed laminar convection from a helical coil", Chemical Engineering Communications 9, pp. 185-200, 1981.
[10] Stine W., Geyer M., "Power from the sun", 2001. [Online]. Available: www.powerfromthesun.net.
[11] Anderson J.D., "Fundamentals of aerodynamics - Fourth edition", McGraw-Hill, 2007.
[12] Raithby G.D., Chui E.H., "A finite-volume method for predicting a radiant heat transfer in enclosures with participating media" Journal of Heat Transfer, Vol. 112, pp. 415–423, 1990.
[13] Chui E.H., Raithby G.D., "Computation of radiant heat transfer on a non-orthogonal mesh using the finite-volume method", Numerical Heat Transfer, Part B, Vol. 23, pp. 269–288, 1993.
[14] ANSYS. FLUENT - Theory guide. 2009.
[15] Patankar S.V., "Numerical heat transfer and fluid flow", Washington D.C., 1980.
[16] Ferziger J. H., Peric M., "Computational methods for fluid dynamics – Third edition", Springer-Verlag, Berlin, 2002.
[17] Versteeg H. K., Malalasekera W., "An introduction to computational fluid dynamics. The finite volume method" Longman Scientific and Technical, Harlow, 1995.
[18] Incropera, F. P., D.P. Dewitt, T.L. Bergman, and A.S. Lavine. Fundamentals of heat and mass transfer, 6th edition. John Wiley & Sons, 2007.
[19] "www.microthermgroup.com," [Online].
[20] "www.schott.com/borofloat/english/?highlighted_text=borofloat," [Online].
[21] Poirazis H., Kragh M., Hogg C., "Energy modelling of ETFE membranes in building applications", 11th International IBPSA Conference, Glasgow, Scotland, July 27-30, 2009.